

**Numerical and experimental investigation of air flow and heat transfer in  
a complete circuit of a hypersonic wind tunnel.**

*Drozdo S.M., Davletkildiev R.A., Rtischeva A.S.<sup>1</sup>*

**Abstract**

This work presents numerical and experimental investigation of high-enthalpy real air flow structure in the complete circuit of TsAGI T-117 hypersonic wind tunnel with account for heat transfer processes in the air cooler and at wind tunnel walls. In the numerical simulation, wind tunnel circuit was modeled as a sequence of axisymmetric segments: a prechamber, a shaped nozzle, a simplified test section, a supersonic diffuser, a chamber preceding the cooler, a semipermeable cooler segment, a chamber after the cooler, and a fragment of the gas exhaust system. In all segments, axisymmetric Navier-Stokes equations for viscous heat-conducting air with a turbulence model were solved using ANSYS Fluent software. Real-gas properties of air were modeled in assumption of equilibrium excitation of O<sub>2</sub> and N<sub>2</sub> vibration modes. The most challenging segment for numerical modeling is the cooler which consists of 1797 individually water-cooled tubes. Two models of air flow through the cooler are considered. The first is the simplified "Darcy" model, in which the cooler is represented as a porous medium. In the second model, "slot channels", the air cooler segment is represented by a set of axisymmetric channels, and convective heat exchange with the cooling water is assumed on their exterior. Results of numerical simulation of gas dynamics in the complete circuit of T-117 wind tunnel and heat transfer processes in the air cooler and at wind tunnel walls, at regimes with Mach number M=7.5 and M=10.5 in the test section, are analyzed in this work. Comparison is made between simulation results and experimental data.

**Keywords:** hypersonic flow, nozzle, test section, air cooler, heat transfer.

**Nomenclature**

M – Mach number,	P – pressure,
T – temperature,	P <sub>0</sub> – total pressure,
T <sub>0</sub> – total temperature,	P' <sub>0</sub> – total pressure behind normal shock,
T1 – static temperature,	P1 – static pressure,
Re – Reynolds number,	G – air-mass flow,
TS – test section of the wind tunnel,	M <sub>c</sub> – Mach number in the flow core.

---

1

*TsAGI, Russia, E-mail: smdrozdov@yandex.ru*

### **Introduction and objectives of numerical modeling.**

Since new hypersonic wind tunnels are planned to be built at TsAGI, the problem of numerical simulation of gas dynamics and heat transfer in all gas circuit elements of this type of experimental facilities becomes topical. Numerical investigations employing up-to-date models of two- and three-dimensional flow and heat transfer of a viscous and heat-conducting gas may help to understand physical processes taking place in the wind tunnel, optimize nozzle contours and structure of the test section, air cooler and gas exhaust systems, and specify parameters of the new facility's working regimes.

The aim of this study was to calculate gas dynamics in T-117 wind tunnel circuit with account for heat transfer processes in the air cooler and at wind tunnel walls, and, based on experimental data obtained in methodological tests in T-117, to verify the mathematical models and calculation procedures required for designing a new experimental facility.

The primary function of a wind tunnel is to create a high-quality stream in the test section with distributions of main parameters (Mach number, dynamic pressure, total temperature and pressure) as uniform as possible. The definitive element in this task is, undoubtedly, the nozzle (Fig. 1); a number of calculation procedures [1, 2] for defining nozzle profiles have long been known and applied with great success.

The next element of a wind tunnel circuit is the test section. In hypersonic facilities, a test section in the form of Eiffel chamber is usually used, in which the central hypersonic jet exiting the nozzle interacts with the slowly moving surrounding gas. Correct modeling of peculiarities of this interaction is essential to determine stream parameters at the location of tested models in the new facility.

The hypersonic stream needs to be efficiently decelerated after the test section. This task is fulfilled by the diffuser, geometrical parameters of which must be chosen to allow supersonic flow through the inlet and the convergent part at all positions of a standard model in the test section, i.e. to ensure diffuser start. Simulation of the diffuser is impossible without knowing flow history in the nozzle and in the test section, but it is also important to specify conditions at diffuser exit where the flow can be subsonic.

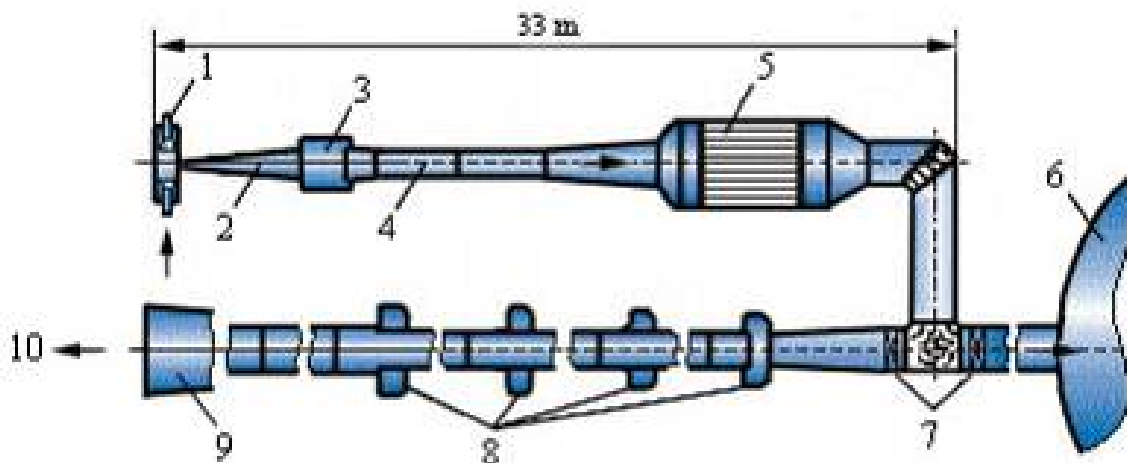


Fig. 1. Scheme of aerodynamic circuit of T-117 wind tunnel.

1 – prechamber and electric arc heater; 2 – nozzle; 3 – test section; 4 – diffuser; 5 – heat exchanger;  
6 – vacuum tank; 7 – vacuum isolation valves; 8 – ejectors; 9 – subsonic diffuser; 10 – noise  
suppression chamber.

It should be noted that simulation of air flow in wind tunnels is usually performed only up to diffuser exit where certain back pressure is imposed. Numerical and experimental investigations carried out in this study showed that the pressure distribution at diffuser exit is substantially non-uniform and depends on flow regime in the air cooler. Consequently, it is incorrect to use fixed pressure as a boundary condition: the air cooler with the preceding chamber and a fragment of gas exhaust channel (Fig. 1) must be included in the numerical model.

A distinctive feature of hypersonic wind tunnels is the presence of a high-enthalpy stream that needs to be formed in the prechamber and the nozzle and then cooled down before reaching the exhaust channel or a vacuum tank. The heat power to be removed from the stream is enormous and, in fact, equal to the power of gas heater in the prechamber (8 to 20 MWatts). For stream cooling, a special air cooler segment is employed. In T-117, the air cooler follows the diffuser and consists of a cylindrical body with an internal diameter of 3.4 m and a length of 4 m uniformly filled with 1797 tubes 51 mm in diameter, through which the air being cooled is flowing (Fig. 1, Fig. 6). Space between the tubes is filled with slowly circulating water.

Simulation of flow and heat transfer in air cooler tubes is complicated by several significant issues, the foremost of which is the uncertainty of gas-dynamic conditions at inlet and outlet of the air cooler, with the latter being a part of aerodynamic circuit that operates in interaction with the diffuser and the gas exhaust channel. This means that inlet and outlet conditions for air cooler tubes can only be determined from the global solution of air flow and heat transfer in the entire wind tunnel circuit. But it is non-realizable to solve a transient problem for a wind tunnel circuit that includes an air cooler with 1797 tubes. Simple estimations show that a computational grid with the minimally sufficient spacial resolution will count a few billion cells. Therefore, to find a global solution, the air cooler segment must be schematized so as to provide acceptable grid size (below 20-30 million cells) while reproducing primary characteristics of the real cooler – the gas-dynamic resistance to the air stream and heat removal through the tube walls. A substantial issue of the calculations is choosing the optimal model of heat exchange between the tubes and cooling water.

In this study, the following approach to numerical simulation of gas dynamics and heat transfer in T-117 wind tunnel circuit is suggested. The geometry of the T-117 circuit's numerical model consists of 7 parts (Fig. 1): 1) a schematized axisymmetric prechamber; 2) an axisymmetric nozzle shaped for the given Mach number; 3) a schematized axisymmetric test section with the volume close to that of the real test section; 4) axisymmetric supersonic diffuser; 5) axisymmetric chamber preceding the cooler; 6) a semipermeable air cooler segment; 7) a chamber after the cooler and a fragment of the gas exhaust system.

In the prechamber, total pressure  $P_0$  and temperature  $T_0$  are specified. In segments 1-7, axisymmetric Navier-Stokes equations for viscous and heat-conducting air with a turbulence model (Spalart-Allmaras or SST) are solved using ANSYS Fluent software. Real-gas properties of air were modeled in assumption of equilibrium excitation of  $O_2$  and  $N_2$  vibration modes and a temperature-dependent heat capacity of the gas mixture  $C_p=f(T)$ . All solid flow-bounding surfaces, except air cooler walls, were assigned a constant temperature of  $T_w=300$  K.

Two models of air flow through the cooler were considered. The first was a simplified model, in which the cooler is represented by a porous medium, and Navier-Stokes equations are extended with volumetric resistance (non-linear Darcy's law) and convective heat transfer between air and the porous base (cooler walls). Resistance and heat transfer parameters in cooler tubes were determined from a series of flow and heat transfer simulations in a single tube at a wide range of inlet and outlet boundary conditions. The Darcy's model allows using a very economical mesh (3-5 million cells) and obtaining solutions in a shorter time with the computing facilities available.

However, only two flow regimes corresponding to conditions of the experiment can be considered in this model: a supersonic regime with deep vacuumization of the wind tunnel's exhaust system, in which the pressure drop along the cooler is positively sufficient to realize a supersonic air flow at cooler tubes outlet; and a subsonic regime with a comparatively small pressure drop, which provides a fully subsonic flow through all cooler tubes.

The general case of air flow through cooler tubes requires a more detailed approach, which in this work is considered with the second model, "slot channels". In this model, air cooler segment is represented by a set of concentric axisymmetric channels, and convective heat exchange with cooling water is assumed on their exterior. Geometric parameters of equivalent axisymmetric cooler channels are determined from the following conditions: equality between total cross section area of the channels and total area of cooler tubes' cross-section at the end wall of the real cooler; uniform permeability throughout the entire volume of the cooler; identity of flow rate through the tubes and through a channel with the same cross-section at the same pressure drop. The computational grid for this model consists of about 15 million cells. Simulation results presented in this work were obtained with the "slot channels" model of air cooler segment. A full cycle of calculations was also performed using the "Darcy" model, and the results were in satisfactory agreement with those obtained using "slot channels".

### **1. Results of air flow and heat transfer simulation in T-117 wind tunnel circuit.**

Numerical investigation of air flow and heat transfer in T-117 wind tunnel circuit was conducted for typical T-117 operating regimes: at  $M=7.42$ ,  $P_0=1613186$  Pa,  $T_0=804$  K,  $P'_0=18035$  Pa; and at  $M=10.5$ ,  $P_0=9140000$  Pa,  $T_0=1187$  K,  $P'_0=20000$  Pa. To verify grid convergence, solution was obtained on two grids: grid G1 and grid G2 with double spacial resolution in each direction (15208000 cells). Results turned out to be practically identical, therefore only calculations with the finer grid G2 are analyzed in what follows.

Figures 2a,b show Mach number distribution in the nozzle and the test section of T-117. Numerical modeling provides highly accurate reproduction of the flow structure: a boundary layer in the nozzle, a uniform flow core at nozzle exit and in the text section, a mixing layer and a recycling zone in the test section, stagnation areas at diffuser walls. Distributions of Mach number, pressure, dynamic pressure and other parameters are uniform across the flow core which is over 640 mm in diameter (Fig. 3). Average Mach number in the core  $M_c=7.423$  is very close to the value of  $M_e=7.48$  registered in experiment. In calculations with the nozzle for  $M=10.5$ , an average value of  $M_c=10.2$  in the flow core was obtained, which is also close to the experimental value of  $M_e=10.3$ .

Figure 3 gives a comparison between calculated and experimental transversal distribution of pressure ratio  $P'_{0i}/P_0$  across the test section at a distance of  $x=[608, 755]$  mm from the nozzle exit where tested models are usually located. It is worth noting that the pressure  $P'_0$  behind normal shock is a quantity that is directly measured in experiment. The agreement can be described as good, especially considering the fact that  $P'_{0i}/P_0$  was calculated from Mach number and static pressure using a perfect gas model ( $C_p/C_v=1.4$ ). Overall, it can be concluded that numerical modeling provides a good reproduction of air flow and heat transfer in T-117's nozzle, test section and the first half of the diffuser.

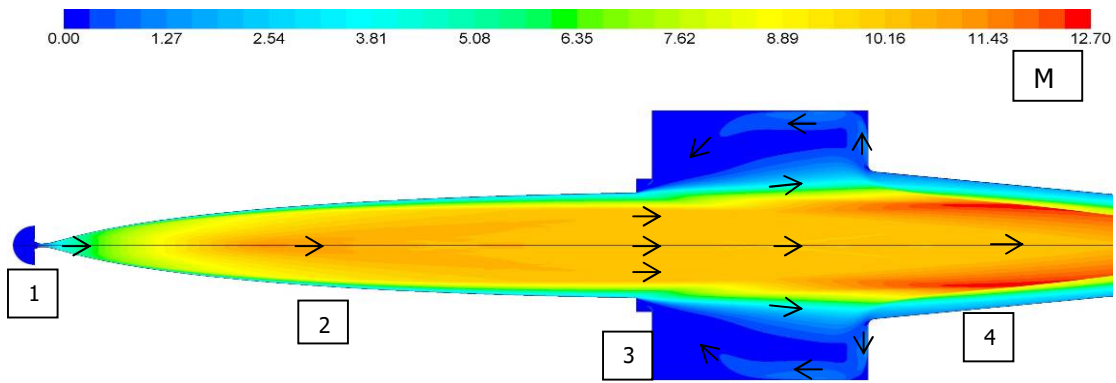
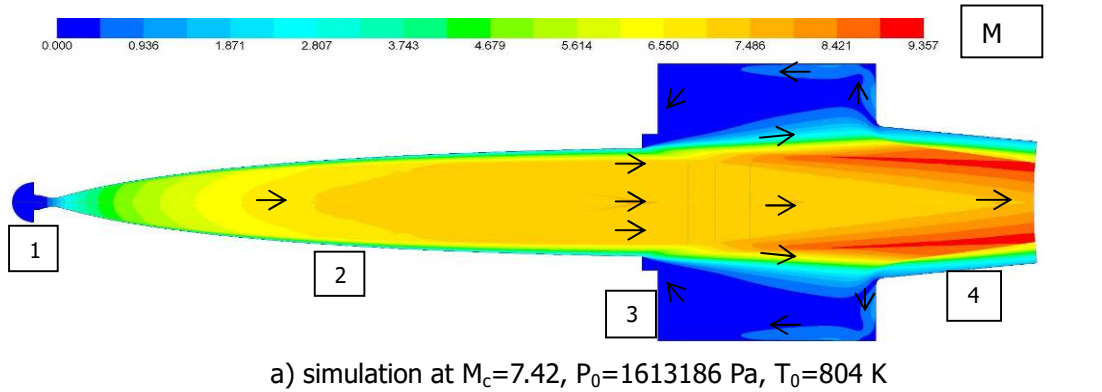


Fig. 2. Distribution of Mach number in T-117 nozzle and test section.  
1 – prechamber, 2 – nozzle, 3 – test section, 4 – diffuser fragment.

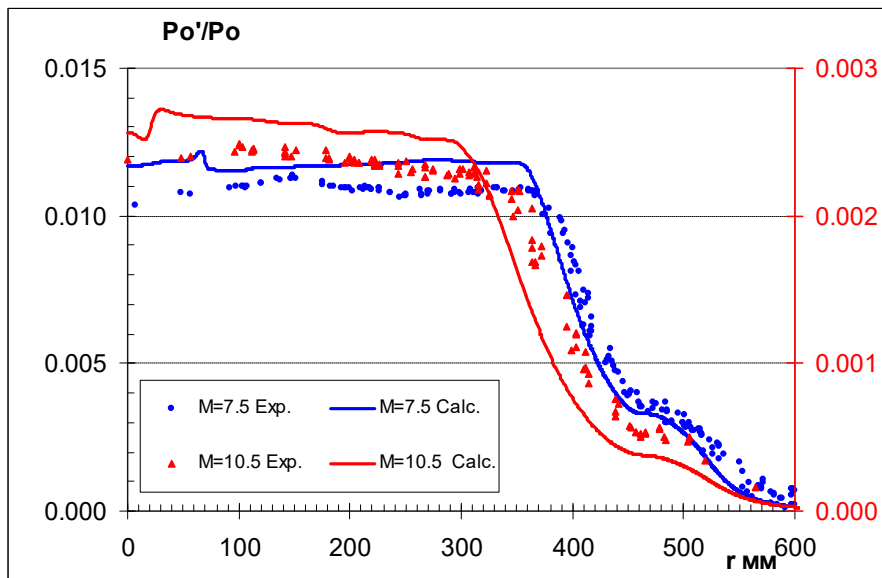
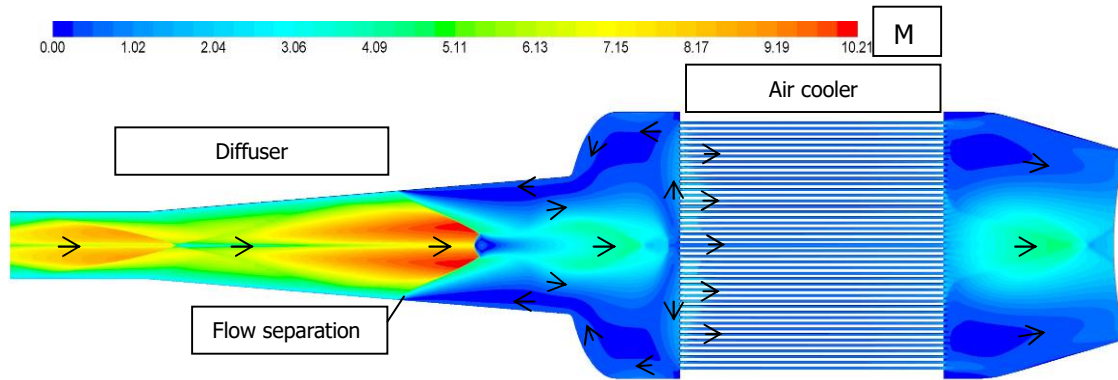


Fig. 3. Comparison of calculated (Calc.) and experimental (Exp.) radial distribution of  $P'_{0i}/P_0$  across the test section. Y-axis for  $M_c=7.5$  is on the left and for  $M_c=10.5$  on the right.

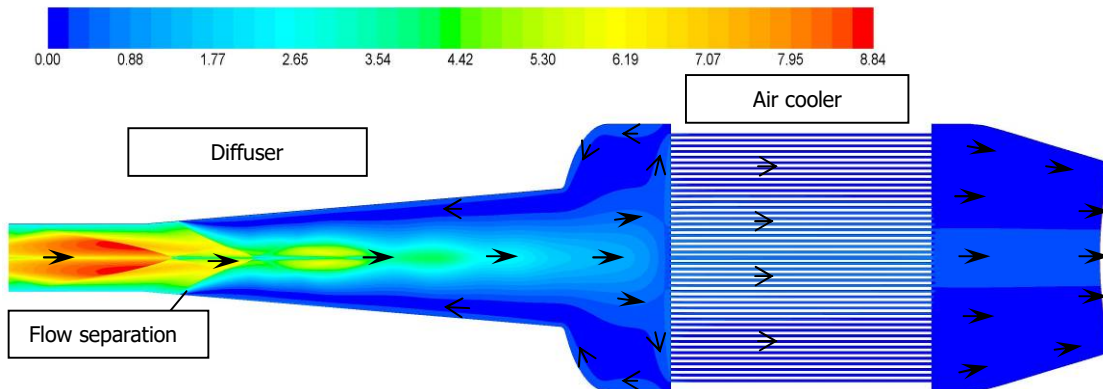
After diffuser start, the flow in the nozzle, in the test section and the diffuser up to its diverging part is supersonic and does not depend on flow conditions in air cooler tubes. But flow type and structure in diffuser's diverging part, in air cooler tubes and further down the stream depends considerably on the counter pressure  $P_e$  realized in gas exhaust channel. Numerical and experimental studies have shown that the main parameter defining flow and heat transfer in the second part of hypersonic wind tunnel circuit is the ratio of  $P_e/P'_0$ . The value of Mach number at nozzle exit and mass rate of flow also influence the flow in the second part of the circuit, but to a much lesser extent. During T-117 operation with exhaust to a vacuum tank, the counter pressure level  $P_e$  gradually increases as the tank is being filled. Therefore, the main results of numerical air flow and heat transfer simulation in the second part of hypersonic wind tunnel circuit are considered at different values of  $P_e/P'_0$ , using the operating mode with Mach number  $M=10.5$  in the test section as example. Two qualitatively different flow regimes were realized in the calculations: a supersonic regime with deep vacuumization of the tank when  $P_e/P'_0 < 1$  and the pressure drop is positively sufficient to realize a supersonic flow in all cooler tubes; and a subsonic regime at  $P_e/P'_0 > 0.2$  with a comparatively small pressure drop, which provides a fully subsonic flow through all cooler tubes. In what follows, both regimes are examined in the divergent part of the diffuser and further down the stream. At supersonic regime, a flow with  $M > 2$  fills almost the entire diffuser, and only near its exit a subsonic separation zone with reverse flow and bow shocks is formed (Fig. 4a). The flow is not entirely steady-state: the separation zone is gradually spreading upstream, and a pulsating reverse flow zone is present near the tunnel axis in proximity of the cooler's front wall. The supersonic stream separated from diffuser walls hits the front wall of the cooler at a Mach number of  $M \approx 4$  and spreads radially while also entering slot channels. At the exit section of almost every air cooler tube (slot), a supersonic flow is realized (Fig. 5a). Flow stagnation in the shocks results in temperature rise and decrease of specific heat ratio  $C_p/C_v$ . Total temperature in the flow core is close to  $T_{0i}/T_0 = 1$  and drops to  $T_{0i}/T_0 \approx 0.8$  in the separation zone. Pressure distribution is substantially non-uniform across the front wall of the cooler and changes by a magnitude of 10 from the maximum of  $P/P'_0 = 1.33$  in the centre to  $P/P'_0 = 0.18$  in peripheral zones. As shown later in this study (Fig. 8a), very similar values of temperature  $T/T_0$  and pressure  $P/P'_0$  were registered in experiment within the first 4-6 seconds of wind tunnel operation.

Now let us examine T-117 operation mode with subsonic air flow through cooler tubes (slots). This mode realizes either when the exhaust ejectors operate at a reduced intensity or during the second half of T-117 run with exhaust into a vacuum tank. Comparison of calculation results for the subsonic regime with those for supersonic air flow from the tubes (Figures 4a, b) demonstrates large qualitative and quantitative differences. First, the zone of flow separation is significantly larger, taking up almost the entire diverging part of the diffuser. Flow core in this area is diminished, Mach number in it gradually decreases, and the flow entering the chamber preceding the cooler is already subsonic. In cooler tubes (Fig. 5b) and in the chamber after the cooler, the flow is subsonic. Static temperature gradually increases in diffuser's diverging part and reaches a maximum of  $T/T_0 \approx 0.9$  near the front wall of the cooler. In cooler slot channels, the temperature decreases due to heat exchange with the walls, with central and peripheral tubes operating under significantly different temperature and heat transfer conditions. With respect to total temperature, a gradual reduction of the flow core (defined by the condition  $T_{0i}/T_0 > 0.9$ ) is observed, owing to interaction with detached flow, cold walls of the diffuser and of the chamber preceding the cooler. Maximum total temperature is  $T_{0i}/T_0 \approx 0.9$  at cooler's front wall and  $T_{0i}/T_0 < 0.46$  after the cooler. At the supersonic regime, temperatures were noticeably higher. Pressure distribution at the front wall of the cooler is more uniform (compared to the supersonic case), with a maximum of  $P_{0i}/P'_0 = 0.55$  and a minimum of  $P_{0i}/P'_0 = 0.27$  in peripheral parts. Pressure and temperature values very close to calculated ones were registered in experiment at 9-12 seconds after wind tunnel start (Fig. 8b, 9b).



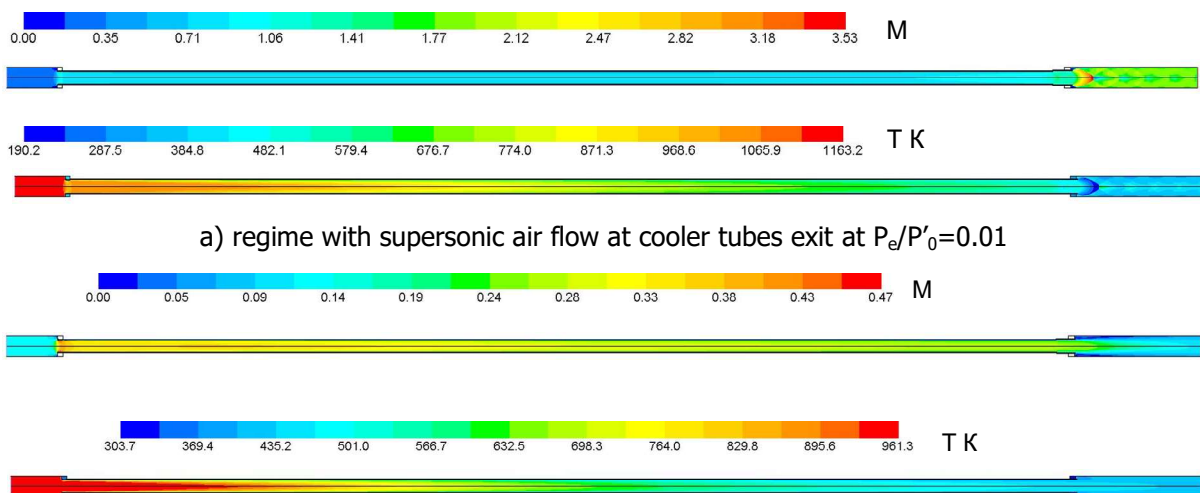


a) regime with supersonic air flow at cooler tubes exit at  $P_e/P'_0=0.01$



b) regime with subsonic air flow at cooler tubes exit at  $P_e/P'_0=0.248$ .

Fig. 4. Mach number distribution in T-117 circuit simulation at Mach number of  $M_c=10.5$  in the test section.



a) regime with supersonic air flow at cooler tubes exit at  $P_e/P'_0=0.01$

b) regime with subsonic air flow at cooler tubes exit at  $P_e/P'_0=0.248$ .

Fig. 5. Air flow and heat transfer simulation in T-117 cooler tubes at Mach number of  $M_c=10.5$  in the test section.

Using pressure and temperature distributions at cooler tubes' inlet and outlet obtained in simulations of the full T-117 circuit, calculations of flow and heat transfer in a separate cooler tube were performed. A coupled problem of gas dynamics and heat transfer was solved numerically, in which the full Navier-Stokes and energy balance equations are considered in a gaseous medium, and the heat conduction equation with a convective heat transfer condition on the outer surface of the tube is solved in the solid volume of tube walls. Figure 5a,b shows contours of Mach number and temperature at two qualitatively different flow regimes in a tube with a Mach number of  $M_c=10.5$  in the test section. Results of numerical simulation of the experimentally realized cooler tube operation mode showed that the tube removes 13.7 kW of thermal power in the central part. For other design modes of cooler operation, the amount of heat absorbed by the tubes varies from 2.5 to 32 kW depending on flow regime realized in the tube.

At supersonic flow regime, total energy flux at the entrance of T-117 computational domain is  $W_{in}=9825608$  W; the cooler takes off  $W_{ac}=-5056907$  W, and walls of the diffuser and of the chamber preceding the cooler absorb  $W_w=-368487$  W. At subsonic regime, the respective values are  $W_{in}=9825608$  W,  $W_{ac}=-4991486$  W,  $W_w=-612888$  W.

Summarizing the comparative analysis of diffuser and air cooler operating regimes, it can be concluded that the subsonic exhaust regime is significantly more efficient in terms of energy consumption (deep vacuumization of the exhaust channel is not required) and substantially softer in terms of thermal effect on the cooling tubes. However, at this regime there is a danger of flow separation spreading into diffuser throat and further into the convergent part, which would cause destruction of hypersonic flow in the test section of the wind tunnel.

## **2. Experimental investigation of air flow and heat transfer parameters distribution in T-117 circuit.**

The aim of experimental investigation was to obtain the necessary amount of experimental data on distributions of stream total pressure in the test section, pressure magnitude before and after air cooler segment and temperatures at inlet and outlet of T-117 cooler tubes to verify the results of numerical investigation.

The object under study in this case was T-117 wind tunnel circuit, in which the following measurements were taken:

- Pressure distribution measurements in the test section with a 21-point total pressure rake (Fig. 6).
- Total pressure (points  $P_{gd1}$ ,  $P_{gd2}$ ,  $P_{gd3}$ ) and total temperature (points  $T_{gd1}$ ,  $T_{gd2}$ ,  $T_{gd3}$ ) in points of the rake before air cooler (Fig. 7).
- Total pressure (points  $P_{gc1}$ ,  $P_{gc2}$ ,  $P_{gc3}$ ) and total temperature ( $T_{gc1}$ ,  $T_{gc2}$ ,  $T_{gc3}$  points) in points of the rake after air cooler.
- Pressure in T-117 vacuum tank ( $P_{vac}$ ).
- Pressure in the Eiffel chamber of the test section ( $P_{ts1}$ ,  $P_{ts2}$ ).
- Three temperature measurement points ( $T_{td1}$ ,  $T_{td2}$ ,  $T_{td3}$ , chromel-alumel thermocouples) at the inlets of three cooler tubes in the central (2), intermediate (4) and peripheral (5) areas of the cooler's front wall (Fig. 7).
- Three temperature measurement points ( $T_{tc1}$ ,  $T_{tc2}$ ,  $T_{tc3}$ , chromel-alumel thermocouples) at the outlets of three cooler tubes in the central, intermediate and peripheral areas of cooler's end wall.
- Two temperature measurement points on the metal surface ( $T_{w1}$ ,  $T_{w2}$ ) on the front wall of the cooler in central and intermediate areas.
- A pressure measurement point ( $P_{stc1}$ ) in the central region of the cooler's front wall between the tubes (Fig. 7); a pressure measurement point ( $P_{stc2}$ ) in the corner of the front and side walls of the cooler; a pressure measurement point ( $P_{stc3}$ ) in a cylindrical niche in the side wall of the cooler.



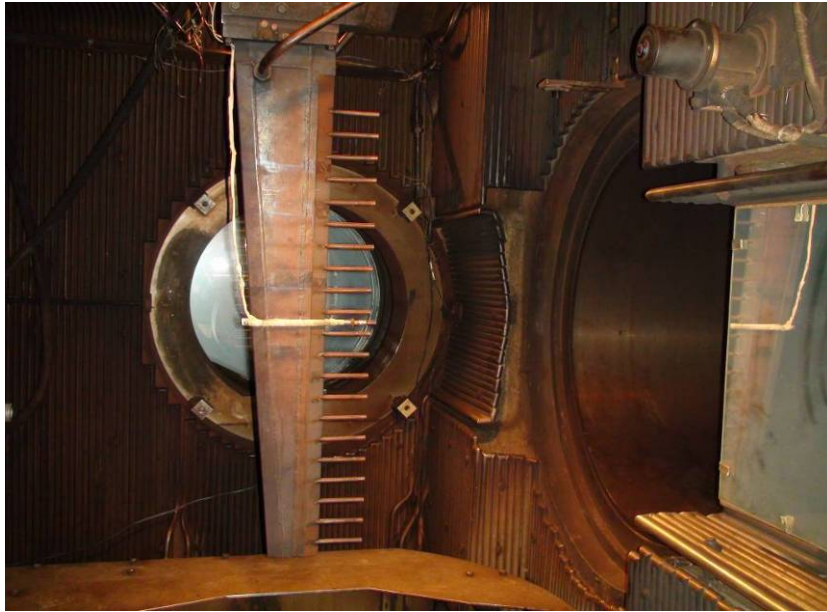


Fig. 6. Total pressure rake in T-117 test section.

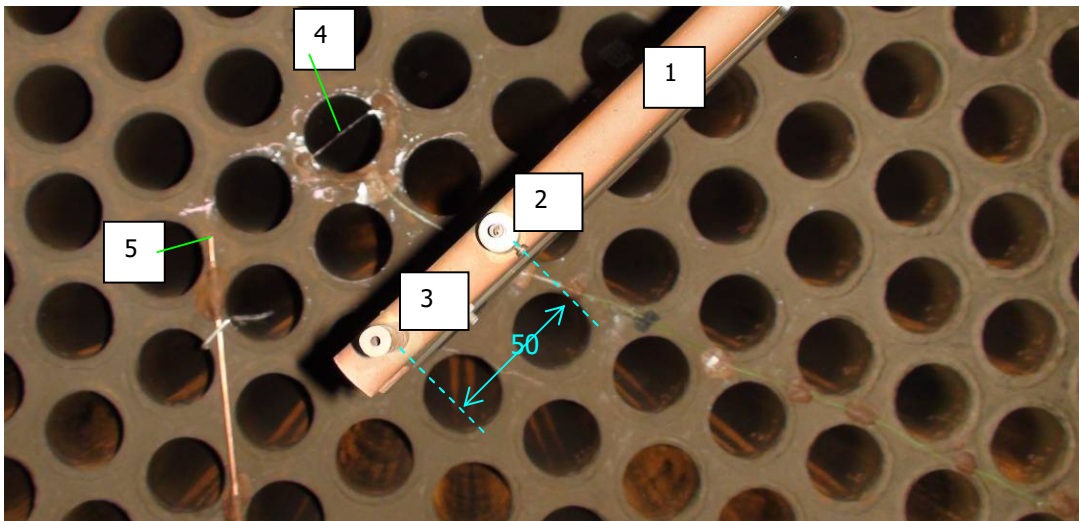


Fig. 7. Measurement rake before T-117 air cooler and measurement points on the front wall of the cooler.

1 – rake, 2 – temperature measurement point ( $T_{gd1}$ ) on the rake, 3 – pressure measurement point ( $P_{gd1}$ ) on the rake, 4 – temperature measurement point ( $T_{td1}$ ) at central cooler tube inlet, 5 – pressure measurement point ( $P_{stc1}$ ) in the central region of the cooler's front wall.

Total pressure and temperature measurements before and after the cooler are performed by special rakes mounted on the wall of the cooler (Fig. 7). Each rake contains three temperature sensors paired with three total pressure heads. Sensor pairs are spread along the rake at a distance of 800 mm from each other, with extreme pressure points ( $P_{gc1}$ ,  $P_{gd1}$  - 3 in Fig. 7) located almost at wind tunnel axis. On the front-wall rake, pressure heads were put at a distance of 480 mm from the front wall of the air cooler, and on the end-wall rake they were situated at a distance of 1150 mm behind the cooler's end wall. Continuous sampling of measurement data at a rate of 100 Hz was performed during the entire wind tunnel run. Table 1 specifies main parameters of the tests carried out in T-117.

Table 1. Parameters of tested regimes.

Run #	$P_{0r}$ , atm	$T_{0r}$ , K	M	$P_{1r}$ , Pa	$T_{1r}$ , K	$P'_{0r}$ , Pa	Re (1 m)	G, kg/s
5524	22.29	714	7.49	335.3	59.3	24444	5796333	14.87
5525	24.06	815	7.48	363.2	68.6	26381	4938667	15.00
5526	49.70	1177	10.47	77.9	54.4	11085	2088692	4.398
5527	48.39	1203	10.45	76.1	55.8	10802	2030203	4.234

Results of transversal flow parameters distribution measurements in the test section at several distances from nozzle exit were given previously when analyzing numerical simulation data (Fig. 3). Pressure and Mach number distributions in the flow core are quite uniform with small deviations from the average values given in Table 1. Flow core diameter is  $D_c=700$  mm at  $M_{ts}=7.4$  in the test section, and  $D_c=620$  mm at  $M_{ts}=10.5$ .

It is of greatest interest to analyze the results of pressure and temperature measurements in T-117 air cooler segment. Fig. 8 shows pressure evolution curves at cooler's front wall ( $P_{stc1}$ ,  $P_{stc2}$ ) and in the vacuum tank ( $P_{vac}$ ). The moment of electric arc ignition in T-117 prechamber was taken as  $t=0$ , after which a specified flow regime was established in the nozzle and in the test section of T-117. During this process, a sharp increase in pressure (2 in Fig. 8) and temperature (Fig. 9) takes place in the central part of cooler's front wall.

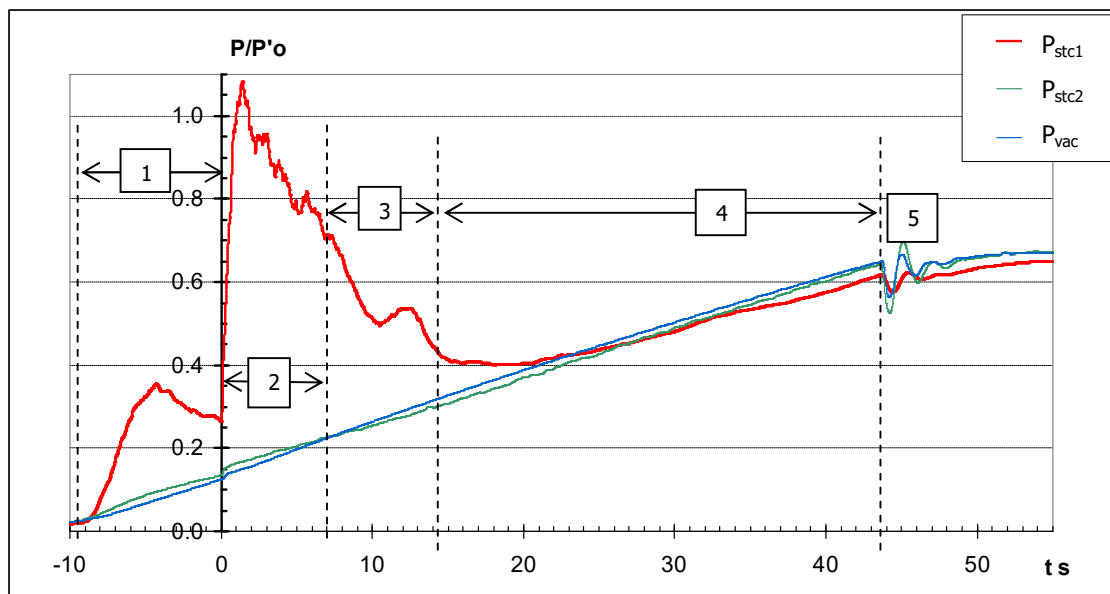
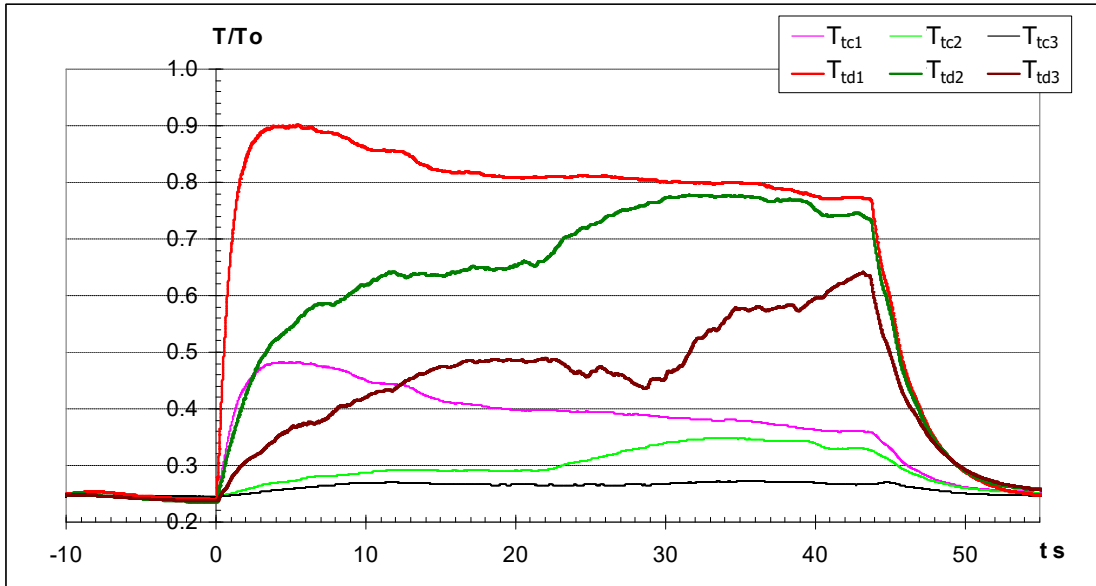


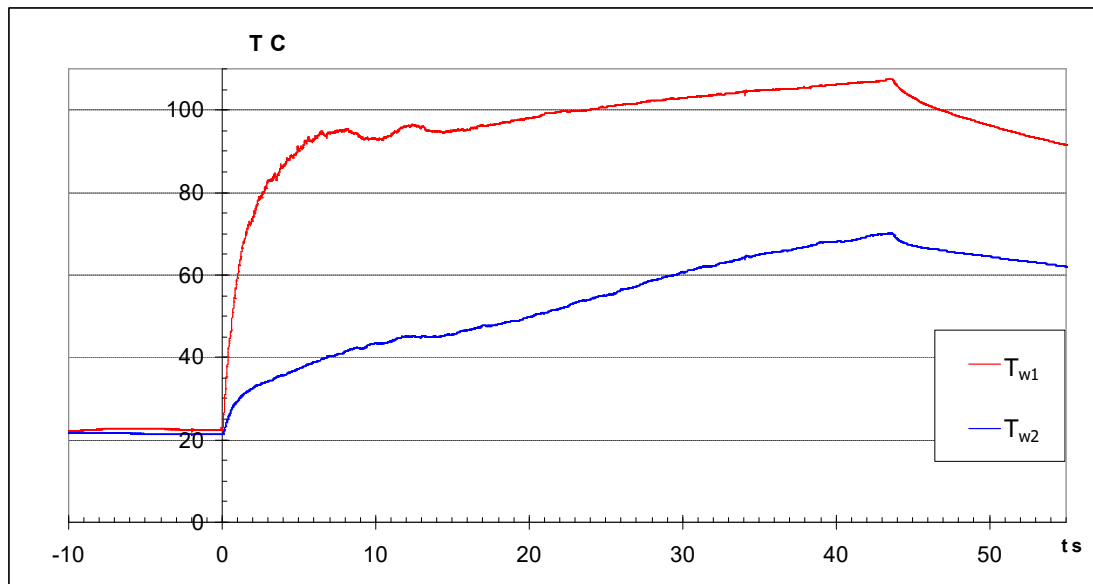
Fig. 8. Run 5527 at  $M=10.5$ , pressure measurements at the front wall of the air cooler ( $P_{stc1}$ ,  $P_{stc2}$ ) and in the vacuum tank ( $P_{vac}$ ). Regimes: 1 – cold stream, 2 – supersonic, 3 – transonic, 4 – subsonic, 5 – stream destruction.

Fig. 9a shows temperature evolution curves in measurement points at the front wall at cooler tubes' inlet ( $T_{td1r}$ ,  $T_{td2r}$ ,  $T_{td3}$ ) and at the end wall at tubes' outlet ( $T_{tc1r}$ ,  $T_{tc2r}$ ,  $T_{tc3}$ ). It is evident that the temperature at central tube's inlet quickly approaches the stagnation temperature. The temperature drop between inlets and outlets of the tubes is approximately  $0.4T_0$ . Note that the thermocouple sensors at cooler tubes and pressure sensors at the front wall of the cooler proved considerably more effective as means of stream parameter measurements than similar sensors on the rakes, which operated under strong flow inclination and displayed understated results.

Temperature measurements on the surface of cooler’s front wall showed that by the end of a long run 5527 the temperature had reached 107° C (Fig. 9b). However, this should not cause the cooling water to boil, since, according to calculations, there is a temperature drop by approximately 20 degrees across tube wall thickness.



a) temperature  $T/T_o$  :  
at tube inlets on the front wall of the cooler ( $T_{td1}$ ,  $T_{td2}$ ,  $T_{td3}$ ),  
at tube outlets on the end wall of the cooler ( $T_{tc1}$ ,  $T_{tc2}$ ,  $T_{tc3}$ ).



b) temperatures of the metallic surface of cooler’s front wall.

Fig. 9. Temperature at different points of T-117 circuit. Run 5527,  $M=10.5$ .

Using the results of both numerical and experimental investigation of flow and heat transfer in T-117 circuit, the following regimes can be distinguished (Fig. 8):

1 - Cold stream before arc ignition (1 in Fig. 8). This is an off-design regime, when partial air condensation occurs in the nozzle and in the test section, and specified Mach number is not realized. A supersonic flow possibly takes place in almost the entire diffuser (up to the front wall of the cooler) and at cooler tubes' outlet. This is indicated by a large pressure drop along the cooler ( $P_{0in}/P_{0out}\approx 4$ ).

2 - Supersonic regime. This regime features a supersonic flow in almost the entire diffuser (up to the front wall of the cooler) with a large pressure drop along the cooler ( $P_{0in}/P_{0out}\approx 6$ ). Supersonic flow is also realized at outlets of most of the cooler tubes during the first 6–8 seconds of wind tunnel operation (2 in Fig. 8). In this case, a relatively short separation zone occurs at diffuser exit and a toroidal vortex forms in the chamber preceding the cooler (Fig. 4a).

3 - Transonic regime (3 in Fig. 8). At this regime, a supersonic flow is maintained in the converging part and at the very beginning of the diverging part of the diffuser. But further down the diverging part, a transition to transonic regime occurs (Fig. 4b). In this case, the separation zone expands and occupies almost the entire diverging part of the diffuser, while a large toroidal vortex is present in the chamber preceding the cooler. Due to a decrease in pressure drop ( $P_{0in}/P_{0out}<2.5$ ), a subsonic flow is formed at outlets of central tubes of the cooler, and a subsonic flow is realized in peripheral tubes.

4 - Subsonic regime (4 in Fig. 8). At this regime, a supersonic flow is maintained only in the converging part of the diffuser. At diffuser throat and at the beginning of the expanding part, a system of shocks is formed and flow velocity reduces to transonic values, which further decrease to small subsonic values in the expanding part of the diffuser and in cooler tubes. The pressure drop along the cooler is relatively small ( $P_{0in}/P_{0out}<1.5$ ). The separation zone covers the entire expanding part of the diffuser, and in the chamber preceding the cooler large and small toroidal vortices are formed.

5 - Flow destruction in the entire T-117 circuit.

## Conclusion

In this work, numerical and experimental investigation of high-enthalpy real-gas air flow structure in the complete circuit of TsAGI T-117 hypersonic wind tunnel with account for heat transfer processes in the air cooler and at wind tunnel walls was conducted. Numerical modelling provides highly accurate reproduction of the flow structure: a boundary layer in the nozzle, a uniform flow core at nozzle exit and in the test section, a mixing layer and a recycling zone in the test section, stream stagnation in the diffuser, flow and heat transfer in the air cooler. Results of numerical simulation are in good agreement with measurement data. Cross-analysis of calculated and experimental results helped to understand flow structure and physical processes taking place during the main flow and heat transfer regimes in T-117 circuit. The developed models of air flow and heat transfer in T-117 will be helpful for simulation of high-enthalpy real-gas flow in circuits of other hypersonic facilities.

## References

1. Alan Pope, Kenneth L. Goin. High-Speed Wind Tunnel Testing. John Wiley & Sons Publ, New York, 1965. (Russ. ed.: Pope A., Goin K. Aerodinamicheskiye truby bolshikh skorostei. Ed. N.N. Shirokov. Moscow, Mir Publ, 1968. 504 p.)
2. Verkhovsky V.P., Nosov V.V. Investigation of flow field in axisymmetric shaped nozzle in Mach number range of  $M=7-10$ . // TsAGI Science Journal, 2004, Vol. 35, No. 2. (In Russian)

